Monitoring and Controlling the Electron Dynamics in Helium with Isolated Attosecond Pulses

Steve Gilbertson,[1] Michael Chini,[2] Ximao Feng,[1] Sabih Khan,[1] Yi Wu,[2] and Zenghu Chang[1,*]

[1]*J. R. Macdonald Laboratory, Department of Physics, Kansas State University, Manhattan, Kansas 66506, USA*

[2]*Departments of Physics and CREOL, University of Central Florida, Orlando, Florida 32816, USA*

(Received 4 June 2010; published 27 December 2010)

Helium atoms in the presence of extreme ultraviolet light pulses can lose electrons through direct photoionization or through two-electron excitation followed by autoionization. Here we demonstrate that, by combining attosecond extreme ultraviolet pulses with near infrared femtosecond lasers, electron dynamics in helium autoionization can be not only monitored but also controlled. Furthermore, the interference between the two ionization channels was modified by the intense near infrared laser pulse. To the best of our knowledge, this is the first time that double excitation and autoionization were studied experimentally by using isolated attosecond pulses.

DOI: 10.1103/PhysRevLett.105.263003 PACS numbers: 33.20.Xx, 32.10.−f, 32.80.Zb

A new era in ultrafast science started in 2001. In that year, attosecond extreme ultraviolet (XUV) pulses were generated for the first time [1,2]. Unlike femtosecond laser pulses that have been widely used for studying nuclear motion, the advent of the attosecond pulse makes it possible to investigate the much faster electron dynamics in atoms and molecules [3–6]. As a proof-of-principle experiment, isolated attosecond pulses have been used to measure the Auger decay time in Kr atoms, which yielded results that agree well with spectroscopy measurements [7], and recently work has been done looking into XUV pump-IR probe experiments in He [8,9].

Since atoms and molecules containing many electrons are the building blocks of matter all around us, understanding the interactions between electrons is one of the basic tasks for atomic physics. Being an atom that has only two electrons, helium is a perfect target for studying correlated electron dynamics for atomic theorists, and autoionization is one of the processes dominated by electron-electron interactions. In the past few years, autoionization has become a hot research topic for theorists again because of the possibility of studying electron-electron interactions in the time domain experimentally [10–14]. The so-called ''Fano profiles'' present in an XUV absorption spectrum from helium were theoretically described in 1961 [15]. When a helium atom in its ground state absorbs an XUV photon with energy of 60.1 eV [see Fig. 1(a)], a single electron can be emitted, leaving the other electron in the ground state, through direct photoionization. Alternatively, both electrons can be excited to the doubly excited $2s2p$ state through absorption of a single photon. The excited state can then ''autoionize'' with one electron returning to the ground state and the other electron being liberated from the atom. The quantum interference between the two paths of ionization gives the characteristic Fano line shape in the spectral domain. The lifetime of the $2s2p$ state estimated from the width of the Fano profile is ~17 fs, which is too fast to be studied in the time domain by using the picosecond synchrotron pulses.

In Fig. 1(b), a helium atom is illuminated with a single isolated ~100 as pulse, which sets the start time of the double excitation. The binding energy of the doubly excited state is 5.3 eV. A 9 fs near infrared laser pulse can affect the electrons in the highly excited states as well as in the continuum states. In this work, we report the first time domain experimental results on autoionization and control over the electron dynamics using isolated attosecond pulses in a pump-probe experiment.

To time resolve the helium autoionization process, we used an attosecond streak camera described in detail elsewhere [16]. Our input laser, a 1.5 kHz, 9 fs, 650 μJ pulse, was split into two components by an 80% transmitting beam splitter. The main portion of the beam passed through double optical gating optics in the collinear configuration [17,18] and was focused to a neon gas filled target. This generated a single isolated attosecond XUV pulse [19]. In the experiments, the carrier envelope phase was unlocked,

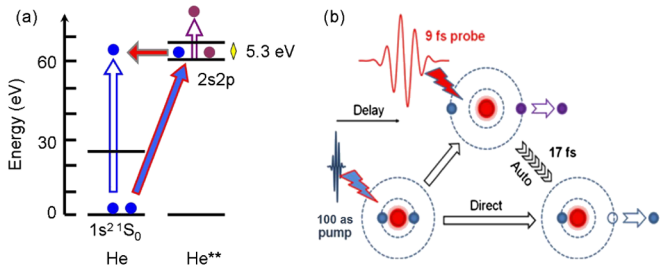

FIG. 1 (color online). Description of the autoionization process. (a) Formation of the Fano profile in helium. An electron in the ground state can be emitted from the parent atom through absorption of a single 60 eV photon (blue and white vertical arrow). Alternatively, the atom can first absorb the 60 eV photon and transit to a doubly excited state (blue arrow). (b) The principle of the pump-probe experiments.

but this had no effect on the results [20]. The isolated XUV pulse was ~100 as in FWHM, characterized by the frequency resolved optical gating for the complete reconstruction of attosecond bursts method using the same setup [21,22]. The reflected portion of the original 9 fs near infrared (NIR) beam recombined with the XUV pulse at the hole drilled mirror. The two beams were focused to a second gas jet filled with helium. The XUV beam generated a photoelectron burst in helium that was collected by a cone of a position-sensitive time-of-flight detector (TOF) aligned along the laser polarization axis. In order to improve the energy resolution of the TOF, a retarding potential was applied in the region between where the photoelectrons were born and where they entered the TOF [23].

Experiments utilizing femtosecond NIR lasers to "steer" electrons generated by attosecond XUV pulses can be qualitatively described by using the strong-field approximation (SFA) [24,25]. More recently, the SFA calculation was extended to describe the formation and decay of an isolated Fano resonance in the presence of a strong NIR laser field [11]. In this model, the XUV attosecond pulse $\vec{E}_x(t)$ simultaneously excites ground state electrons to the discrete resonance and to continuum states with momentum $\vec{p}$ through the dipole transition $\vec{d}(\vec{p})$. The resonant state then autoionizes into the continuum with decay amplitude given by $\frac{\Gamma}{2}(q-i)e^{-iE_r t-\Gamma t/2}$, where E_r is the resonance energy and Γ is the resonance width. The parameter q indicates the relative probability of excitation to the resonant state and direct photoionization to the continuum. Finally, both the direct photoionized and autoionized electrons propagate in the NIR field. In our approach, the SFA was further modified to take into account the depletion of the population of the autoionizing state by the NIR field.

The amplitude of the continuum electron on the TOF with momentum $\vec{p}$ as $t \to \infty$ is given in atomic units by

$$b_L(\vec{p},\tau) = i\int_{-\infty}^{\infty} dt \int_{t}^{\infty} dt' \vec{E}_x(t-\tau)\vec{d}[\vec{p}-\vec{A}(t)]e^{itI_p} \left\{a(t-t')\frac{\Gamma}{2}(q-i)\exp\left[-\left(iE_r+\frac{\Gamma}{2}\right)(t'-t)\right] + i\delta(t'-t)\right\}\exp\left[-i\int_{t'}^{\infty}\frac{[\vec{p}-\vec{A}(t'')]^2}{2}dt''\right], \quad (1)$$

where $\vec{A}(t)$ is the vector potential of the NIR laser and τ is the delay between the XUV and NIR pulses. E_r is the resonance energy, and Γ is the resonance width. The parameter q indicates the relative probability of excitation to the resonant state and direct photoionization to the continuum. $|a(t)|^2$ describes the change of the population in the $2s2p$ state by the NIR laser pulse. To determine the population of the doubly excited state, the Perelomov-Popov-Terent'ev model for multiphoton ionization was used [26]. The ionization probability was calculated at each delay, and the decay amplitude was inserted into Eq. (1). The resulting spectrogram was obtained by convolution with the TOF energy resolution for a typical XUV pulse reconstructed in the presence of a NIR field 9 fs in duration and with peak intensity of 7×10^{11} W/cm^2.

Figure 2(a) shows a smoothed surface profile plot of the measured data. The inset in Fig. 2(a) is the mirror reflectivity curve used in the experiments. This explains the large signal strength at ~40 eV. The $2s2p$ autoionization resonance occurs at 60.1 eV in photon energy or 35.5 eV in photoelectron energy (the ionization potential of helium is 24.6 eV). The amplitude of the Fano peak of the autoionization resonance as a function of delay is plotted in

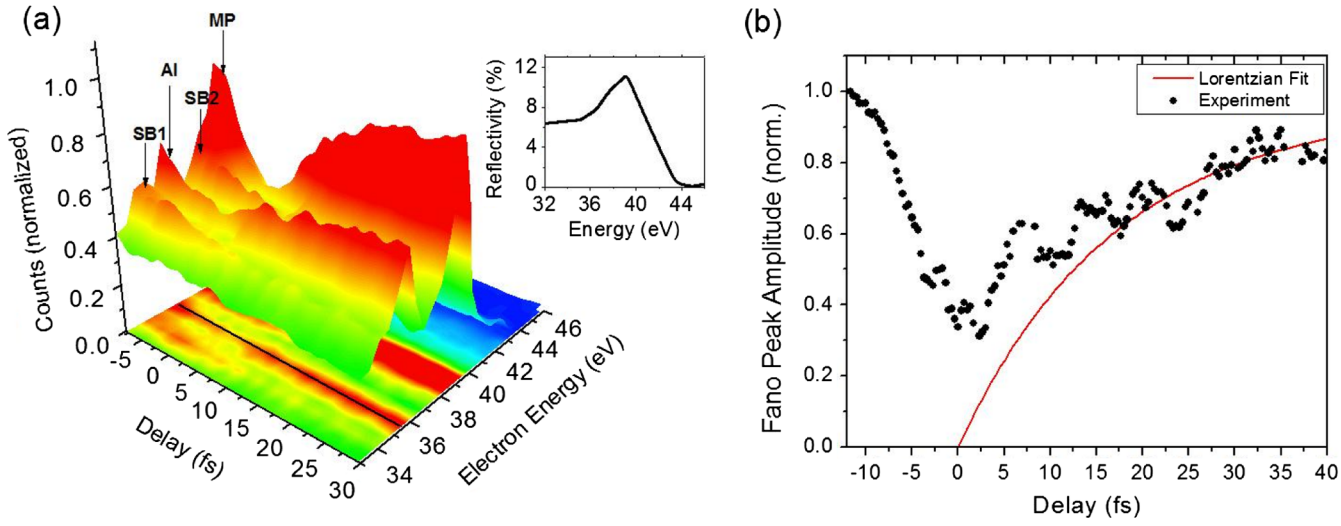

FIG. 2 (color online). Surface plot of a streaked spectrogram and autoionization Fano peak amplitude. (a) The electron spectra as a function of delay following the perturbed autoionization process. The inset shows the mirror reflectivity over the region of interest. The arrows indicate the locations of the sidebands (SB1 and SB2), the autoionization resonance (AI), and the peak reflectivity of the mirror (MP). (b) The autoionization signal as a function of delay for a 35.5 eV photoelectron.

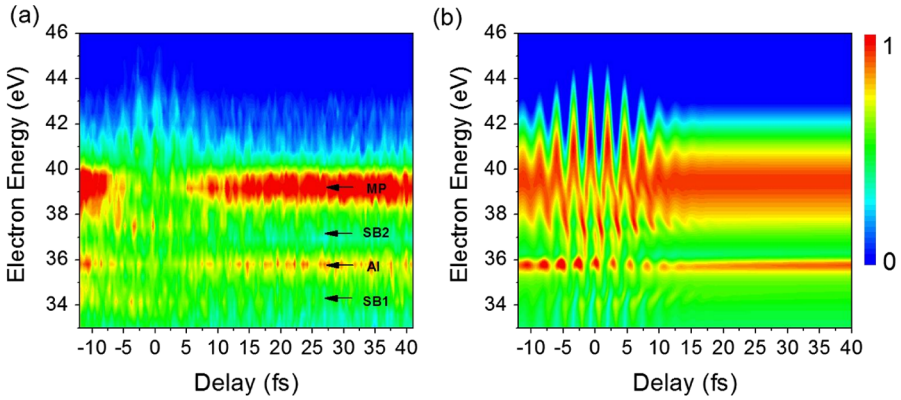

FIG. 3 (color online). Experimental and simulated streaked spectrograms. (a) The measured electron spectrogram. The arrows indicate the locations of the sidebands (SB1 and SB2), the autoionization resonance (AI), and the peak reflectivity of the mirror (MP). (b) A simulated electron spectrogram using a modified version of the SFA. The 9 fs IR streaking laser pulse is centered at $\tau = 0$. In the calculation, the XUV transform limited pulse duration was 90 as, and the NIR intensity was 7×10^{11} W/cm^2.

Fig. 2(b). Figure 3(a) shows a spectrogram of the projection of the data in Fig. 2(a), which can be directly compared with the simulated results shown in Fig. 3(b).

The measured and simulated spectrograms show a common feature. Sidebands above and below the Fano peak show up when the NIR laser is present. One sideband (SB1) is a 1.5 eV downshift, while the other (SB2) is a 1.5 eV upshift, where 1.5 eV is the NIR photon energy. The appearance of the sidebands can be explained by the absorption or emission of an NIR photon by the autoionized electron, which has already been predicted by Zhao and Lin [11].

It is clearly seen that the Fano peak height varies with the time delay. The signal along the line at 35.5 eV in the projection of the surface plot is shown in Fig. 2(b). This is the total counts of the data set integrated over the width of the $2s2p$ resonance, smoothed, and plotted as a function of delay. The height is reduced with the two pulses overlapped, and the reduction shows a distinct asymmetry about delay $\tau = 0$. For negative values of delay, for which the NIR laser arrives first, the signal decreases quite sharply. For positive delay, however, the signal increases more slowly and follows the autoionization decay.

The reduction of the Fano peak height can be explained by the depletion of the doubly excited state by the NIR laser field. Because the $2s2p$ state is only 5.3 eV below the continuum, multiphoton ionization by the NIR field can easily deplete the population of the autoionizing state. When the attosecond XUV and NIR pulses overlap, the process will be modified in the following way: After the XUV pulse populates the doubly excited state, some portion of the electron wave packet will be ionized by the NIR field, and fewer autoionized electrons will be detected. The amount that the doubly excited state is depleted depends on the delay, since electrons born into the doubly excited state at different delays will interact with different amounts of the NIR field. The simulations confirm the argument. Mapping the signal of the autoionization resonance peak as a function of delay gives the lifetime of the doubly excited state. From the minimum in the signal, a curve representing the Lorentzian lifetime of the resonance has been fit to the experimental data, seen as the solid red line in Fig. 2(b). The curve is drawn assuming the lifetime is 17 fs. The data represent the first time domain measurement of the lifetime of the autoionization process.

The maximum reduction of the Fano peak depends on the NIR laser intensity. Figure 4(a) shows the experimentally obtained values (black squares) of the minimum of the autoionization resonance. Also shown are the calculated values of the population remaining in the doubly excited state from the Perelomov-Popov-Terent'ev model. Both data sets are normalized to the population of the field-free autoionization resonance. This result demonstrates control over the Fano interference channel by manipulating the autoionization channel.

Control over the Fano interference by the direct ionization channel was also demonstrated. For a particular value of NIR intensity, a plot of the autoionization signal as a function of delay is shown in Fig. 4(b). The strong modulation with the same optical period as the NIR field represents the control over the direct ionization process in autoionization. The attosecond streaking principle states that liberated photoelectrons can be given a momentum shift from a NIR laser with the shift being proportional to the instantaneous vector potential of the NIR field [27]. For arbitrarily flat spectral shapes, this means that just as many photoelectrons can be shifted into some particular energy as are shifted out. However, typical XUV photon-reflecting mirrors and spectra are rarely so flat. The inset in Fig. 2(a) shows the reflectivity curve for the mirror used in the experiments. Above the location of the autoionization resonance at 60.1 eV, the mirror reflectivity has a peak. This gives the opportunity for photoelectrons from higher energies to be shifted into the autoionization resonance more readily than are shifted away from it for certain NIR-XUV delays. Local maxima in Fig. 4(b) represent photoelectrons being streaked from the high reflectivity portion of the mirror [see the inset in Fig. 2(a)] into the

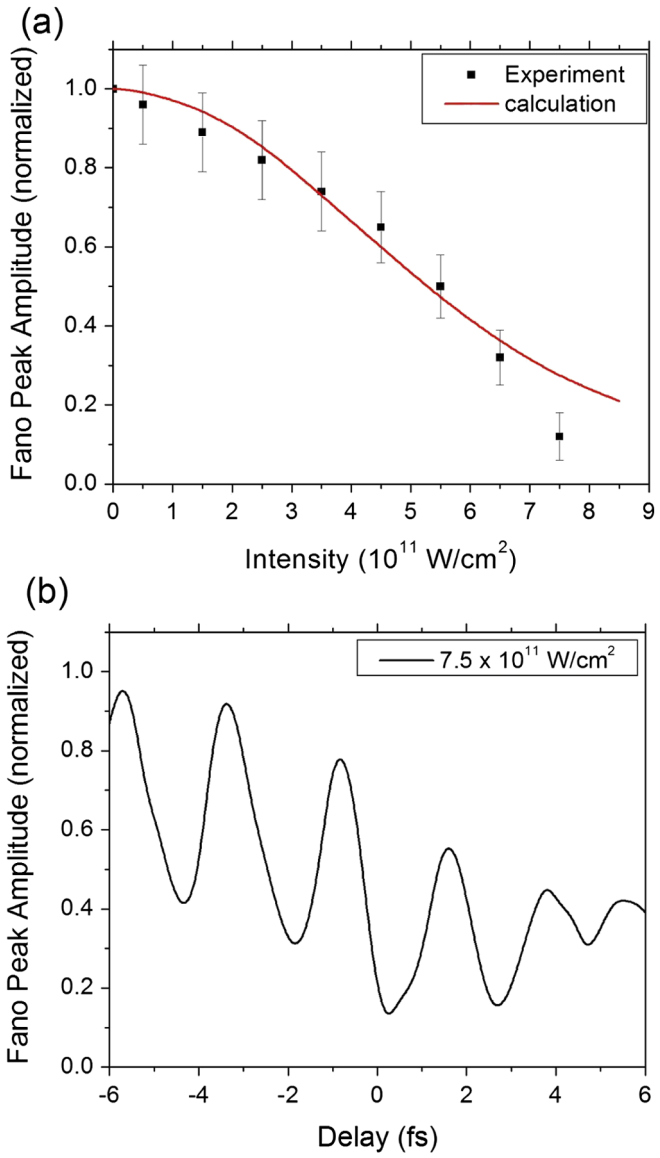

FIG. 4 (color online). Control of the 35.5 eV electron dynamics with intense laser pulses. (a) Dependence of the autoionization resonance signal on the NIR laser intensity. The black squares indicate the minimum signal of the experimental results, normalized to the population of the field-free case. The calculated values (red curve) represent the strength of the autoionization peak. (b) For a particular value of NIR intensity, the population as a function of delay is indicated for an experimental result.

resonance, while minima represent photoelectrons streaked away from it.

Because the resonance strength is determined by the coupling of the doubly excited channel with the direct channel, Fig. 4(b) therefore indicates that the interference effect can be controlled by changing the ratio of electrons from the direct ionization to the doubly excited electrons. This implies that, for certain values of delay, the autoionization resonance can be enhanced even above the field-free case or reduced below the depletion level of the doubly excited state alone.

In this work, we have demonstrated control over both the direct ionization channel and the double excitation channel in the helium autoionization process. This changes the coupling strength between the quantum interferences of the two channels, thereby modulating the strength of the Fano resonance. The time domain lifetime of the $2s2p$ resonance was also measured for the first time. The lifetime of 17 fs agrees well with previous spectral estimates. This work clearly indicates the observation and manipulation of electron dynamics with attosecond pulses and will benefit the theoretical analysis that has been waiting several years for the experimental techniques to reach the current level.

This material is supported by the U.S. Army Research Office under Grant No. W911NF-07-1-0475, by the NSF under Grant No. 0457269, and by the Chemical Sciences, Geosciences, and Biosciences Division, U.S. Department of Energy.

*To whom all correspondence should be addressed.
zechang@mail.ucf.edu

[1] M. Hentschel *et al.*, Nature (London) **414**, 509 (2001).
[2] P. M. Paul *et al.*, Science **292**, 1689 (2001).
[3] E. Goulielmakis *et al.*, Science **317**, 769 (2007).
[4] M. Uiberacker *et al.*, Nature (London) **446**, 627 (2007).
[5] R. Kienberger *et al.*, Nature (London) **427**, 817 (2004).
[6] M. F. Kling *et al.*, in *Proceedings of the Conference on Lasers and Electro-Optics (CLEO), San Jose, California, 2008* (Optical Society of America, Washington, DC, 2008), paper JFH1.
[7] M. Drescher *et al.*, Nature (London) **419**, 803 (2002).
[8] L. Argenti and E. Lindroth, Phys. Rev. Lett. **105**, 053002 (2010).
[9] J. Mauritsson *et al.*, Phys. Rev. Lett. **105**, 053001 (2010).
[10] X. M. Tong and C. D. Lin, Phys. Rev. A **71**, 033406 (2005).
[11] Z. X. Zhao and C. D. Lin, Phys. Rev. A **71**, 060702(R) (2005).
[12] T. Morishita, S. Watanabe, and C. D. Lin, Phys. Rev. Lett. **98**, 083003 (2007).
[13] M. Wickenhauser *et al.*, Phys. Rev. Lett. **94**, 023002 (2005).
[14] T. Mercouris, Y. Komninos, and C. A. Nicolaides, Phys. Rev. A **75**, 013407 (2007).
[15] U. Fano, Phys. Rev. **124**, 1866 (1961).
[16] X. Feng *et al.*, Phys. Rev. Lett. **103**, 183901 (2009).
[17] H. Mashiko *et al.*, Phys. Rev. Lett. **100**, 103906 (2008).
[18] S. Gilbertson *et al.*, Appl. Phys. Lett. **92**, 071109 (2008).
[19] I. J. Sola *et al.*, Nature Phys. **2**, 319 (2006).
[20] S. Gilbertson *et al.*, Phys. Rev. Lett. **105**, 093902 (2010).
[21] Y. Mairesse and F. Quere, Phys. Rev. A **71**, 011401(R) (2005).
[22] H. Mashiko *et al.*, Opt. Lett. **34**, 3337 (2009).
[23] X. Feng *et al.*, Opt. Express **18**, 1316 (2010).
[24] M. Kitzler *et al.*, Phys. Rev. Lett. **88**, 173904 (2002).
[25] J. Itatani *et al.*, Phys. Rev. Lett. **88**, 173903 (2002).
[26] A. M. Perelomov, V. S. Popov, and M. V. Terent'ev, Sov. Phys. JETP **23**, 924 (1966).
[27] E. Goulielmakis *et al.*, Science **305**, 1267 (2004).